On the Higgs Fit and Electroweak Phase Transition

Weicong Huang,[1,][*] Jing Shu,[1,][†] and Yue Zhang[2,][‡]

[1]*State Key Laboratory of Theoretical Physics and Kavli Institute for*
Theoretical Physics China (KITPC), Institute of Theoretical Physics,
Chinese Academy of Sciences, Beijing 100190, P. R. China
[2]*International Center for Theoretical Physics, Trieste 34014, Italy*

(Dated: June 28, 2013)

Abstract

We consider the Higgs portal through which light scalars contribute both to the Higgs production and decay and Higgs effective potential at finite temperature via quantum loops. The positive Higgs portal coupling required by a strongly first order electroweak phase transition is disfavored by the current Higgs data if we consider one such scalar. We observe that by introducing a second scalar with negative Higgs portal coupling, one can not only improve the Higgs fits, but also enhance the strength of first order EWPT. We apply this mechanism to the light stop scenario for electroweak baryogenesis in the MSSM and find a light sbottom could play the role as the second scalar, which allows the stop to be relatively heavier. Non-decoupled effects on the Higgs or sbottom self-interactions from physics beyond MSSM are found to be indispensable for this scenario to work. A clear prediction from the picture is the existence of a light sbottom (below $200\,\mathrm{GeV}$) and a light stop (can be as heavy as $140\,\mathrm{GeV}$), which can be directly tested in the near future.

[*]Electronic address: huangwc@itp.ac.cn
[†]Electronic address: jshu@itp.ac.cn
[‡]Electronic address: yuezhang@ictp.it

I. INTRODUCTION

This year has witnessed the announcement of the Higgs boson discovery by the ATLAS [1] and CMS [2] collaborations. A crucial test of the electroweak symmetry breaking (EWSB) mechanism is to precisely measure the Higgs couplings to the other Standard Model (SM) particles. A SM-like Higgs measurement can put indirect constraints on new physics [3–13] close to the electroweak scale if they couple to the Higgs field. Once those constrains have been obtained, we shall start to explore opening questions related to EWSB.

One big question falls into the above category is the fate of electroweak baryogenesis (EWBG) [14]. In this scenario, baryon asymmetry is generated at the electroweak scale through sphaleron transitions where a strongly first order electroweak phase transition (EWPT) is required to create the departure from equilibrium and prevent the wash out of baryon asymmetry. Therefore, the nature of EWPT would serve as the first window to test the viability of EWBG. The SM is known to fail to provide the above condition and new physics must be introduced through the Higgs portal. Since our current data from LHC on the Higgs production and decay already suggest the preferred parameter space of Higgs couplings from their global fits, it is natural to map the nature of EWSB at the zero temperature to the one at the high temperature, and seek for the impact on EWBG.

Generally, new physics that connect LHC Higgs signal to EWPT can manifest in several ways. New scalars could contribute to both processes through the virtual loop effects (see Fig. 1), or via the mixings with the Higgs boson [15]. The simplest example which triggers a strongly first order EWPT is to add a scalar field S coupling to the Higgs. Consider the general scalar mass term

$$m_s^2(\phi, T) = m^2 + \Pi_s(T) + \alpha\phi^2 \, , \tag{1}$$

where $\Pi_s(T)$ is the thermal self-energy correction to S. The thermal contributions to the Higgs effective potential $V(\phi, T)$ include a negative mass cubic term $-Tm_s^3(\phi, T)/12\pi$. At the critical temperature T_c when $\alpha > 0$, this term is the only dominant source which decreases with ϕ. Its competition with the other ϕ-increasing terms develops a second degenerate nonzero vacuum for $\phi = v_c$. In fact, this lies at the heart of the light stop scenario for EWBG in the MSSM [17].

Meanwhile, if S is a colorful or electric charged particle, the same portal will also modify the effective hgg and $h\gamma\gamma$ couplings and affect the global fit of the Higgs data. The connection is shown in Fig. 1. For the 125 GeV Higgs boson discovered, LHC has seen fewer events in $h \to b\bar{b}, \tau^+\tau^-$ and some excess in $h \to \gamma\gamma$ channel than SM predictions. Improving the Higgs global fit over the SM favors a suppressed production and enhanced di-photon branching ratio. This requires $\alpha < 0$ for S [18], which indicates a tension between EWPT and LHC Higgs signal [19].

The purpose of this work is to examine this tension and seek for possible solutions. Indeed, we can relieve this tension in a generic framework with two scalars S_1 and S_2. The first one S_1 has $\alpha_1 > 0$ and facilitates a first order EWPT through its thermal corrections to $V(\phi, T)$. The second one S_2 has $\alpha_2 < 0$, which not only improves the global fit of the current Higgs data through its destructive contribution with S_1 and the top loop, but also *further enhances the strength of EWPT* (characterized by v_c/T_c). We define a quantity $F[m_s]$ which measures the contribution to v_c/T_c from different scalar fields and show this effect exists in a large parameter space of $\alpha_{1,2}$ and $m_{s_{1,2}}$ (see Fig. 5). Consequently, we expect this mechanism could be widely applied in models of this kind, which include the most popular example,
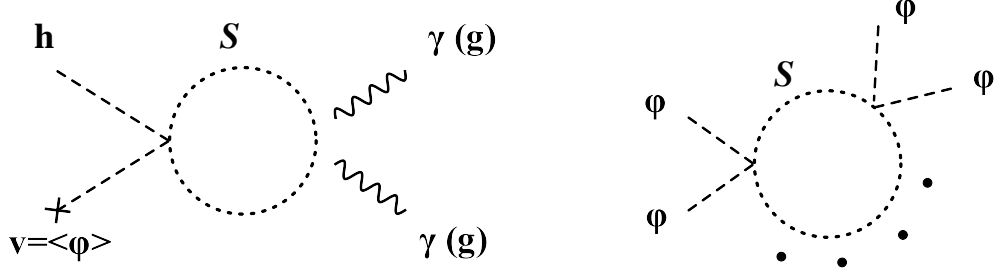
2

FIG. 1: Left panal: Contribution of exotic scalar S to the Higgs coupling to photons and gluons. Right panel: thermal contribution from S loop to the Higgs potential at high temperature.

Minimal Supersymmetric Standard Model (MSSM).

This paper is organized as follows. In the next section, we survey the current status of the global fit to the Higgs data, and the impact of multiple new scalars through the Higgs portal. In section III, we study the role of the scalars in EWPT, and propose a framework where the tension is relieved between the Higgs fit and strong EWPT, with two scalars having similar mass but opposite Higgs couplings. In section IV, we try to implement this framework in the supersymmetric SM, and realize the constraints within the minimal model. We discuss possible solutions by extending the MSSM and emphasize the testability of this scenario at the LHC.

II.   HIGGS FIT WITH NEW COLORED STATES

In this section, we discuss the impact on the fit to Higgs data of new states that couple to the Higgs boson. We start by considering a generic tree-level potential

$$V(H,S) = -\mu^2 H^\dagger H + \lambda(H^\dagger H)^2 + m^2 S^\dagger S + \kappa(S^\dagger S)^2 + 2\alpha(H^\dagger H)(S^\dagger S) , \qquad (2)$$

where S is a complex scalar, carrying electric charge Q_s and number of colors $N(r_s)$, and α characterizes the interaction between the S and the SM Higgs doublet H (with neutral component ϕ). At zero temperature, after electroweak symmetry breaking, $\langle \phi \rangle = v = 246\,\text{GeV}$, the S mass is

$$m_s^2 = m^2 + \alpha v^2 . \qquad (3)$$

The interaction between S and the Higgs boson h is

$$\mathcal{L}_{\text{int}} = -2\alpha v h S^\dagger S . \qquad (4)$$

In calculating the production and decay of the Higgs boson, we have to include the new contribution from this exotic state S loop. This modifies the corresponding rates, which can be parametrized as [12]

$$\frac{\sigma(gg \to h)}{\sigma(gg \to h)_{\text{SM}}} = \frac{\Gamma(h \to gg)}{\Gamma(h \to gg)_{\text{SM}}} = \frac{\hat{c}_{g,\text{SM}} + \delta c_g}{\hat{c}_{g,\text{SM}}}, \qquad \frac{\Gamma(h \to \gamma\gamma)}{\Gamma(h \to \gamma\gamma)_{\text{SM}}} = \frac{\hat{c}_{\gamma,\text{SM}} + \delta c_\gamma}{\hat{c}_{\gamma,\text{SM}}} . \qquad (5)$$

The SM coefficients, from t, $W^\pm$, b loops, are $\hat{c}_{g,\text{SM}} = 0.97$, $\hat{c}_{\gamma,\text{SM}} = -0.81$, repsectively [12]. The new physics correction due to the S loops are

$$\delta c_g = \frac{C(r_s)}{2} \frac{\alpha v^2}{m_s^2} A_s(\tau_s) , \qquad \delta c_\gamma = \frac{N(r_s)Q_s^2}{24} \frac{\alpha v^2}{m_s^2} A_s(\tau_s) , \qquad (6)$$
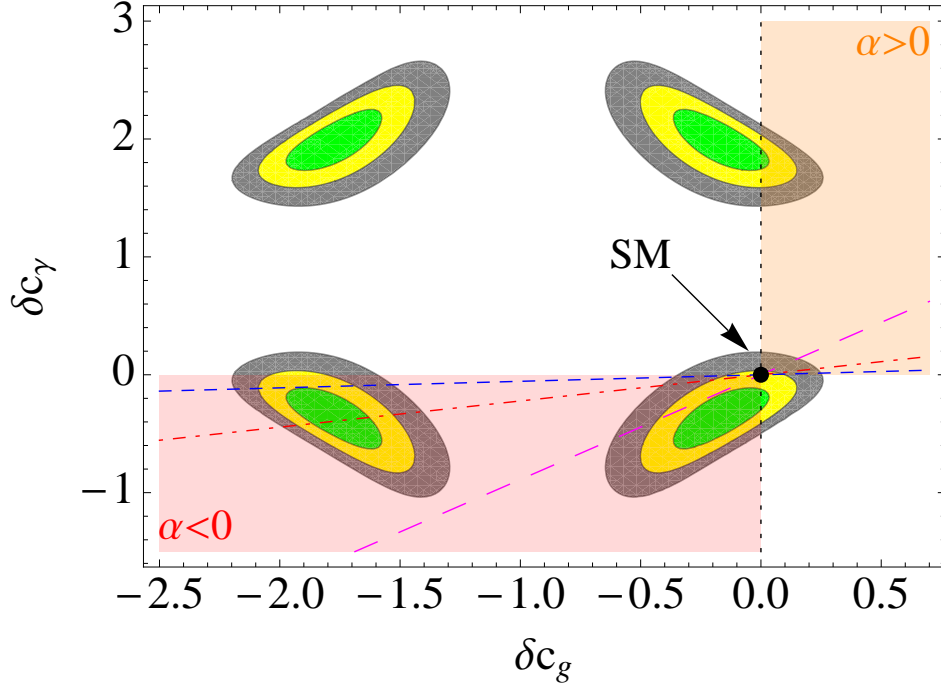
3

FIG. 2: The fit to the LHC Higgs signal in a general two parameter $(\delta c_g, \delta c_\gamma)$ model. The $1, 2, 3\sigma$ region are show as the green, yellow and gray regions. The colored lines represent the trajectory when a new colored state near the electroweak scale is introduced. Red/Blue/Magenta line: color triplet with $Q_s = 2/3, -1/3, -4/3$ respectively. Black (vertical) line: color singlet with $Q_s = -1$.

where $\tau_i = m_h^2/4m_i^2$, and $A_s(\tau) = 3[f(\tau)\tau^{-2} - \tau^{-1}]$,

$$f(\tau) = \begin{cases} 11, & \tau \leq 1 \\ 22, & \tau \geq 1 \end{cases} \tag{7}$$

$C(r)$ is the quadratic Casimir of the color representation, $\mathrm{Tr}(T^a T^b) \equiv C(r)\delta^{ab}$. Notice we have the relations $\delta c_g = (9/2, \ 2, \ 0)\, \delta c_\gamma/Q_s^2$, for color representations **8, 3, 1**, respectively.

Clearly, in order to enhance the $h \to \gamma\gamma$ decay rate or to suppress the $gg \to h$ production, we need $\alpha < 0$ [20].

In order to quantify the fit to the Higgs signals, we define the χ^2,

$$\chi^2 = \sum_{\text{channels}} \frac{(\mu_i - \hat{\mu}_i)^2}{\sigma_i^2} \ , \tag{8}$$

where μ_i is the signal rate calculated in new physics models normalized to the SM one [5] ($\hat{\mu}_i \pm \sigma_i$ are the central value and uncertainty measured by experiments)

$$\mu_i = \frac{\sum_p \sigma_p(c_g, c_\gamma)\zeta^i}{\sum_p \sigma_{p,\text{SM}}\zeta^i} \times \frac{\mathrm{Br}(h \to i)(c_g, c_\gamma)}{\mathrm{Br}(h \to i)_{\text{SM}}} \ , \tag{9}$$

where σ_p is the production cross section of the channel p, ζ_i is the cut efficiency for a particular final state i. In the fit, we take into account of the data released recently in
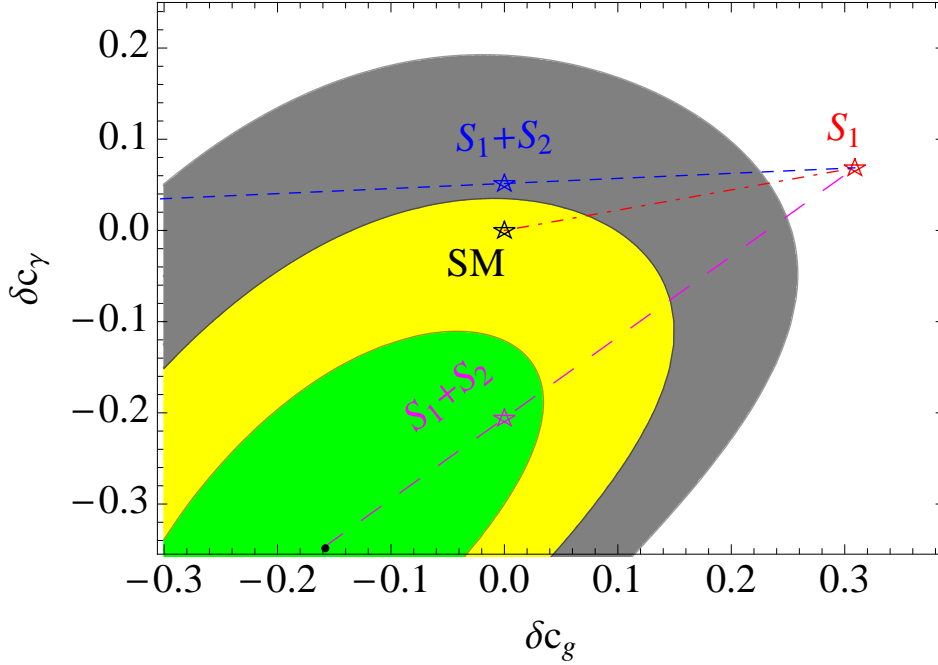
FIG. 3: Black star: SM fit. Red star: the fit with one color triplet scalar with electric 2/3 (stop-like), $m_1 = 120\,\text{GeV}$ and $\alpha_1 = 0.5$. Blue/Magenta star: adding another color triplet with charge $-1/3$ (sbottom-like) or $-4/3$ (exotica), and mass $m_2 = 120\,\text{GeV}$ and $\alpha_2 = -0.5$. We find the $Q_{s_2} = -4/3$ state makes the fit even beter than the $-1/3$ one. This is because it can more than overcome S_1 in δc_γ and make additional negative contribution. Here we have assumed no Higgs invisible decay channels open.

Refs. [1, 2]. Throughout the discussion, we assume the Higgs boson has no invisible decay channels. For exceptions, see [21].

In Fig. 2, we show the regions that can fit the Higgs signal in a general two parameter $(\delta c_g, \delta c_\gamma)$ model. There are four degenerate minimum of χ^2. The SM fit lies between 1σ and 2σ, and can be improved when there are both negative contributions to δc_g and δc_γ. We also show the trajectories that new physics models can cover by adding a single particle with particular color and electric charge quantum numbers, with varying mass and Higgs coupling α. With a light charged scalar (along the dotted vertical line, in black), like the stau, a negative and sizable α clearly profits the fit.

Such global fit can be used to constrain new physics scenarios that enter through the Higgs portal. There have been recent analysis in [22–24] showing the measured Higgs signal at LHC brings severe tension to the light stop scenario for EWBG in the MSSM. The main obstacle is the top squark (stop) contributes to the Higgs effective couplings δc_g and δc_γ constructively with the top quark, as they do in the QCD/QED beta functions [26]. A very light top squark (stop) [25], as required by a strongly first order EWPT, largely enhances δc_g toward an experimentally disfavored direction. This is the tension mentioned in the introduction. In Fig. 3 we quantify the current status of this tension, in the presence of a single stop-like scalar S_1, with $\alpha_1 \approx 0.5$ and mass $120\,\text{GeV}$. Clearly, the fit (red star) is well outside the 3σ region.

This tension can be relieved in two ways. First, if S_1 is allowed to be heavier without weakening the strength of EWPT, the red star will move toward the SM one (in black), and the fit is improved. In fact, we find it crosses the 3σ contour when m_{s_1} is relaxed to around $130\,\text{GeV}$.

Second, an additional colored scalar S_2 may coexist with S_1 near the electroweak scale. If S_2 lies in the same color representation as S_1, and satisfies $m_{s_2} \approx m_{s_1}$ and $\alpha_2 \approx -\alpha_1 < 0$, its contribution to the δc_g will cancel completely that of S_1 and the fit can be significantly improved, as shown in Fig. 3.

In the next section, we will study the impact on EWPT in the presence of an S_2 with $\alpha_2 < 0$. We show that it can assist S_1 (with $\alpha_1 > 0$) and further enhance the phase transition, thus allow the latter to be substantially heavier (the star points in Fig. 3) . In other words, the same S_2 can help to achieve both of the above solutions. This serves as the main point of this work.

It is natural to expect multiple light color/charged states in new physics models. For example, in supersymmetric theories, there are all the scalar partners of quarks and leptons. When some are light, there could be rich parameter space for them to collaborate and improve the harmony between Higgs fit and EWPT.

III.   ENHANCING THE STRENGTH OF PHASE TRANSITION

As discussed in the introduction, the same coupling α defined in Eq. (2), controls the interaction of scalar S with the Higgs boson h, or the high temperature field ϕ. Therefore, it could not only modify the Higgs boson production and decay properties, but also contribute to the finite temperature Higgs potential (Fig. 1), thus play a role in the EWPT.

In order to understand the impact of S in the phase transition, we consider the leading terms in the thermal Higgs potential

$$V(\phi, T) \approx \frac{1}{4}\lambda\phi^4 + \frac{1}{2}\left[-\mu^2 + \Pi_h(T)\right]\phi^2 - T\left[E_{\text{SM}}\phi^3 + 2N(r_s)\frac{m_s^3(\phi, T)}{12\pi}\right] \ . \quad (10)$$

At high temperature, the masses receive thermal corrections

$$\begin{aligned}
m_h^2(\phi, T) &= -\mu^2 + 3\lambda\phi^2 + \Pi_h(T) \ , \\
m_s^2(\phi, T) &= m^2 + \alpha\phi^2 + \Pi_s(T) \ ,
\end{aligned} \quad (11)$$

where the thermal mass corrections are $\Pi_h \approx (6\lambda + 2N(r_s)\alpha + (9g^2 + 3g'^2)/4 + 3y_t^2)\,T^2/12$, $\Pi_s \approx ((2N(r_s) + 2)\kappa + 4\alpha + 4C_2(r_s)g_3^2)\,T^2/12$, with the second quadratic Casimir defined as $T^a T^a = C_2(r)\mathbf{1}$, and satisfies $N(r)C_2(r) = 8C(r)$. For the moment, we neglect the radiative corrections to the effective potential, $\grave{a}$ la Coleman-Weinberg, and high order terms in m/T for the simplicity of illustration, which will be included later in the numerical studies. The thermal mass cubic potential term arises from the daisy resummation and the zero modes of the bosonic fields in the loop [27]. The critical temperature T_c is defined when two local minima become degenerate. One is the symmetric phase and the other is with non-vanishing ϕ. The height of the barrier between the two vacua is determined by the ϕ cubic term.

We focus first on the case $\alpha > 0$, and solve the degenerate minima conditions, $V(0, T) = V(\phi, T)$ and $V'(\phi, T) = 0$. This leads to

$$\frac{N(r_s)}{6\pi}T_c\left[m_s^3(v_c, T_c) - m_s^3(0, T_c)\right] + \frac{1}{4}\lambda v_c^4 = \frac{1}{2}T_c E_{\text{SM}}v_c^3 + T_c\frac{N(r_s)}{12\pi}\frac{\partial m_s^3(v_c, T_c)}{\partial v_c}v_c \ , \quad (12)$$

where $v_c = \langle \phi \rangle$ is the vacuum expectation value (VEV) at the critical point.

Therefore, the strength of EWPT or v_c/T_c depends on the SM part E_{SM} and the quantity

$$F[m_s] \equiv \frac{\partial m_s^3(v_c, T_c)}{\partial v_c} v_c - 2 \left[m_s^3(v_c, T_c) - m_s^3(0, T_c) \right]. \tag{13}$$

E_{SM} arises mainly from SM gauge boson contributions and is known to be too small. The presence of new scalars can enlarge this coefficient if its coupling to the Higgs field α is sufficiently large. We make the requirement $v_c/T_c \gtrsim 0.9$, in order to sufficiently suppress the sphaleron rate in the broken phase, so the following condition should be satisfied

$$\frac{\text{Tr}\left[N(r_s) F[m_s] \right]}{v_c^3} \gtrsim 1.2 \left(\frac{m_h}{125\,\text{GeV}} \right)^2, \tag{14}$$

where the Tr is a sum over all the diagonal elements of the scalar particle mass matrix. For $\alpha > 0$, the thermal potential term proportional to $-T m_s^3(\phi, T)$ decreases as ϕ grows, therefore can balance the other positive terms, and facilitate the development of degenerate vacua of the ϕ field around the critical temperature. In order for this effect to be significant, the thermal mass square should be dominated by the αv_c^2 term. See [17, 28] for the explicit examples.

We point out, interestingly, $F[m_s]$ is always positive, for

$$m_s^2(v_c, T_c) = (m^2 + \Pi_s(T_c)) + \alpha v_c^2, \tag{15}$$

and α taking arbitrary sign. For this quantity to be large enough, as demanded by strong phase transition, one can find solutions for both positive and negative α (see Fig. 4).

This fact, in together with the discussion of Higgs fit improvement in the last section, motivated us to look into the case $\alpha < 0$, for its possible impact on the phase transition. With $\alpha < 0$, the mass cubic term $-T m_s^3(\phi, T)$ grows with ϕ. Therefore, with S itself the degenerate minima or first-order phase transition cannot happen. Namely, with such S itself the equation $V'(\phi, T) = 0$ has not solution at non-zero ϕ, if the condition for building the barrier, $V''(0, T) > 0$, is to be fulfilled at the same time.

However, in the environment of degenerate minima created by the other fields, the presence of such S can further enlarge the ratio v_c/T_c. This picture can be realized if there are multiple relevant particles during the phase transition.

As an example, we introduce two color triplet particles S_1, S_2, with electric charges $2/3$ and $-1/3$ respectively. We fix the parameters $\alpha_1 = 0.5$, $m_{s_2} = 130\,\text{GeV}$ and vary the others, α_2 and m_{s_1}. Here S_1 is designed to mimic the light stop in the MSSM. For $\alpha_2 > 0$, the self interactions of $S_{1,2}$ are fixed to be $\kappa_1 \approx \kappa_2 \approx g_3^2/6$. For $\alpha_2 < 0$, we take into account of the constraint that the zero-temperature potential should be bounded from below at infinity, and modify the value of κ_2 to satisfy $\kappa_2 > \alpha_2^2/\lambda$, which deviates from the MSSM value. The Higgs self interaction $\lambda = 0.13$ is fixed by its mass $125\,\text{GeV}$, and κ_2 is bounded from above ($\sqrt{4\pi}$) by perturbativity. These in turn gives a lower limit $\alpha_2 \gtrsim -0.7$.

In the numerical calculation, we have taken into account of the Coleman-Weinberg potential, V_{CW}, as well as the higher order logarithmic terms in the finite temperature potential, δV_T. They are

$$V_{\text{CW}}(\phi) = \sum_B n_B \frac{m_B^4(\phi)}{64\pi^2} \left[\ln \frac{m_B^2(\phi)}{\Lambda^2} - c \right] + (-1) \sum_F n_F \frac{m_F^4(\phi)}{64\pi^2} \left[\ln \frac{m_F^2(\phi)}{\Lambda^2} - c \right],$$

$$\delta V_T(\phi, T) = -\sum_B n_B \frac{m_B^4(\phi)}{64\pi^2} \left[\log \frac{m_B^2(\phi)}{T^2} - c_B \right] + \sum_F n_F \frac{m_F^4(\phi)}{64\pi^2} \left[\log \frac{m_F^2(\phi)}{T^2} - c_F \right], \tag{16}$$
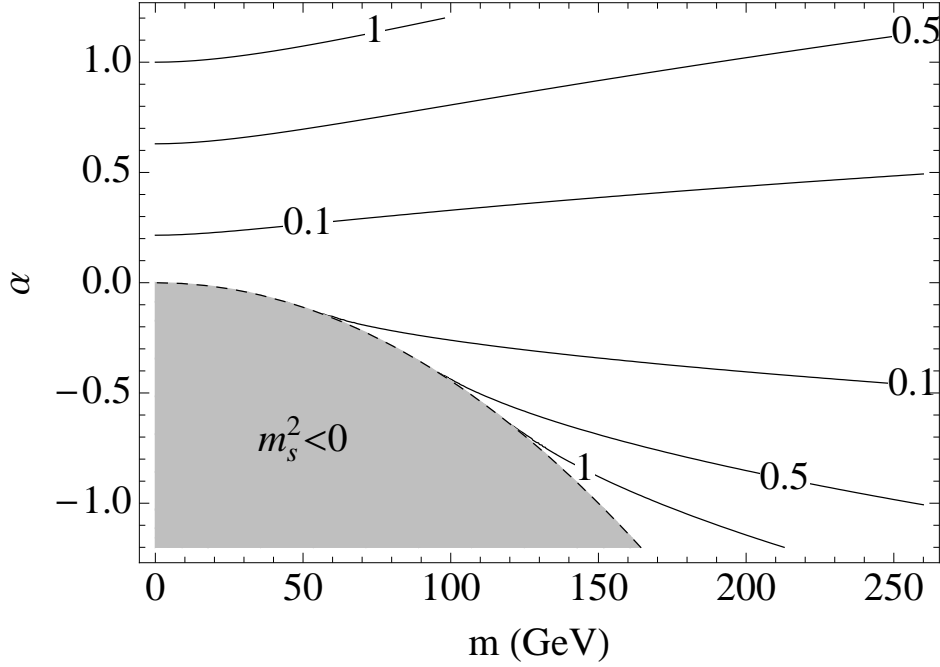
FIG. 4: $F[m_s]$ in units of v_c^3, as a function of parameters $m = \sqrt{m_s^2 - \alpha v^2 + \epsilon_s T^2}$. Here the sample value of v_c is taken to be $150\,\text{GeV}$. One can see $F[m_s]/v_c^3 \sim \mathcal{O}(1)$ can be achieved for either positive α and small m^2, or negative α with low values of $m_s^2(T)$.

where $c_B = 5.41$, $c_F = 2.64$, $c = 3/2$ for scalar and fermions, and $5/6$ for gauge bosons. The total potential is therefore

$$V_{\text{tot}}(\phi, T) = V(\phi, T) + V_{\text{CW}}(\phi) + \delta V_T(\phi, T) \; . \tag{17}$$

We realize the analysis relying on the high temperature expansion at this precision may be subjected to corrections from e.g., two-loop corrections [29] and the issue of gauge dependence [30–32], and leave a more complete analysis to a future study.

Fig. 5 shows the contours of the ratio v_c/T_c. When $\alpha_2 = 0$, we find the strong phase transition condition $v_c/T_c \gtrsim 0.9$ is satisfied at $m_{s_1} \lesssim 120\,\text{GeV}$. This reproduces the result found in Ref. [25]. On top of this, introducing a positive α_2 will further enhance the ratio as expected.

An interesting feature we want to highlight is, in the case $\alpha_2 < 0$, stronger phase transition is also achievable. This is due to the positiveness of $F[m_s]$ – an additional scalar with any sign of α may strengthen the phase transition, as long as it is already made first order. This enhancement can also be qualitatively understood as follows. Around the critical temperature, the S_1 mass cubic term (with large enough α_1) in the thermal potential drags $V(\phi)$ down toward the second minimum. Meanwhile the S_2 cubic term operates in the opposite direction and tends to postpone this to happen, until it drops out from the thermal potential (real part). This leads to a larger value for the critical VEV v_c.

In order for the barrier between $\phi = 0$ and $\phi = v_c$ minima to be built, we again impose the criterion $V''(\phi = 0, T) > 0$, which also helps to remove the appearance of additional local minimum [33]. This sets another relevant lower bound on α_2 (see Fig. 5). It in turn
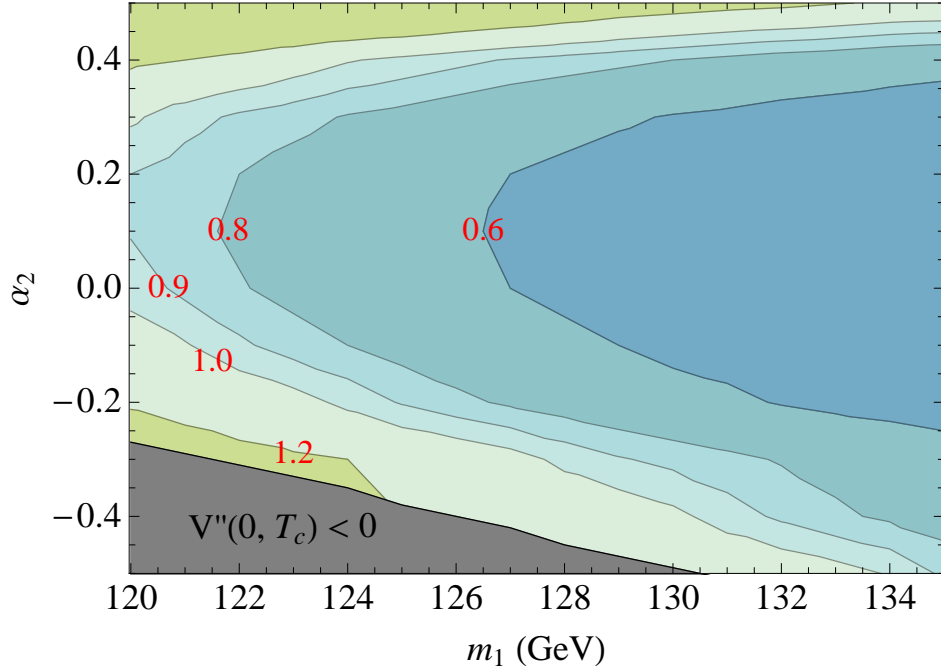
FIG. 5: The ratio of v_c/T_c in a toy model with two color triplet scalars S_1 and S_2 coupling to the Higgs field. We fix $\alpha_1 = 0.5$, $m_{s_2} = 130\,\text{GeV}$ and vary m_1, α_2. It turns out $v_c/T_c > 0.9$ can be achieved for both positive and negative α_2, when $m_{s_1} > 120\,\text{GeV}$. The gray region is excluded because the condition $V''(\phi = 0, T_c) > 0$ is violated.

implies an upper bound on v_c/T_c for negative α_2. There is also an upper bound on the mass of the second scalar, $m_{s_2} < 1.8\,T_c$, which is roughly $200\,\text{GeV}$. This has to be satisfied in order for the distribution of S_2 not to be Boltzmann suppressed in the plasma.

We find for $\alpha_2 \approx -0.5$, the mass of S_1 can be enlarged up to 135–$140\,\text{GeV}$, while maintaining EWPT strong. These features are clearly welcome by the Higgs global fit, as discussed in the previous section.

We notice that in Fig. 5, the contour of v_c/T_c is shifted upwards and minimal value of phase transition strength for a given m_1 is around $\alpha_2 \sim 0.1$. The reason for this asymmetric position of the v_c/T_c contour can be attributed to the impact of α_2, which appears in the thermal masses of Higgs boson, Goldstones, and the scalar S_2. Their masses can be generally parametrized as

$$m^2 \sim m^2 + \frac{1}{12}(\alpha_2 + \dots)T^2 + \alpha_2 v^2 \tag{18}$$

like Eq. (15) where we have highlighted the α_2 contribution via temperature and the electroweak VEV. After daisy resummation, this is the mass that appears in the thermal cubic potential. The $\alpha_2 v^2$ term, if dominate the thermal mass, makes additional contribution to the ratio v_c/T_c, while the $\alpha_2 T^2$ part tends to dilute this effect. There is a competition between the two effects, and numerically this leads to the shift/asymmetry observed in Fig. 5.

9

IV. AN APPLICATION TO MSSM AND BEYOND

At this point, one is certainly tempted to consider the realization of the above framework in supersymmetric theories, especially in view of the tension observed recently between the Higgs fit and the light stop window for EWBG [19, 22–24]. One would expect additional light colored scalar (e.g., the sbottom, see below) with similar mass to the stop but opposite couplings to the Higgs boson. Such light sbottom plays double roles, i.e., to improve the fit to Higgs data and to strengthen the EWPT. Notice that a light sbottom may also contribute to the equilibrium transportation and CP violation sources in EWBG [34].

Hereafter, we assume the other components in the Higgs sector, H, A, $H^{\pm}$, are much heavier than the lightest scalar h. In the decoupling limit, the tree-level couplings of h to weak gauge bosons and fermions are the same as in the SM.

A. Light sbottom assisted light stop scenario

We first briefly review the light stop scenario for a strong EWPT. The mass matrix for stops $(\tilde{t}_L, \tilde{t}_R)$ is

$$\begin{bmatrix} m_Q^2 + m_t^2 + D_L^t & y_t \phi(A_t \sin\beta - \mu\cos\beta) \\ y_t\phi(A_t\sin\beta - \mu\cos\beta) & m_U^2 + m_t^2 + D_R^t \end{bmatrix} , \qquad (19)$$

where $m_t(\phi) = y_t\phi\sin\beta$ and for a given fermion f, the D-term mass $D^f = (T_f^3 - Q_f s_W^2)\cos(2\beta)M_Z^2$. In the limit $m_Q \gg m_U$, the light stop mass is

$$m_{\tilde{t}_1}^2 \approx m_U^2 + D_R^t + y_t^2\sin^2\beta\left(1 - \frac{X_t^2}{m_Q^2}\right)\phi^2 \quad \Rightarrow \quad \alpha_{\tilde{t}_1} = y_t^2\sin^2\beta\left(1 - \frac{X_t^2}{m_Q^2}\right) , \qquad (20)$$

where $X_t = A_t - \mu\cot\beta$. The heavier stop mass is $m_{\tilde{t}_2} \approx m_Q$, much larger than the electroweak scale. We take $\tan\beta \gg 1$ and $X_t \ll m_Q$ throughout the paper. During the electroweak phase transition, $\tilde{t}_1$ contributes to the mass cubic potential term in Eq. (10). The thermal mass is $m_{\tilde{t}_1}^2(\phi, T) = m_{\tilde{t}_1}^2 + \Pi_R(T)$. The light stop scenario for strong electroweak phase transition corresponds to the condition [17], $m_U^2 + \Pi_{\tilde{t}_R}(T) \approx 0$, or $m_U^2 < 0$. In this case, the high temperature mass $m_{\tilde{t}_1}^2(\phi, T) \approx y_t^2\sin^2\beta\phi^2$, and the top Yukawa coupling is large enough to deliver $v_c/T_c \gtrsim 0.9$. An upper bound on the zero-temperature light stop mass is found in [25], which is around $120\,\text{GeV}$. As discussed in Sec. II, this brings confliction with the current Higgs data.

In order to get out of this dilemma, we apply the framework discussed in the previous sections and bring in additional light colored scalar with $\alpha < 0$. In the MSSM, the only possible candidate is the sbottom. Their mass matrix in the basis of $(\tilde{b}_L, \tilde{b}_R)$ is

$$\begin{bmatrix} m_Q^2 + m_b^2 + D_L^b & y_b\phi(A_b\cos\beta - \mu\sin\beta) \\ y_b\phi(A_b\cos\beta - \mu\sin\beta) & m_D^2 + m_b^2 + D_R^b \end{bmatrix} , \qquad (21)$$

where $m_b(\phi) = y_b\phi\cos\beta$. Notice the same m_Q appears, because $\tilde{b}_L$ and $\tilde{t}_L$ belong to the same $SU(2)_L$ doublet. Therefore the heavier sbottom has mass $m_{\tilde{b}_2} \approx m_Q$ and will be nearly degenerate with the heavier stop. A crucial difference from the stop case is that, large coupling to the Higgs VEV can be only obtained through large sbottom mixings, i.e.,

$X_b = A_b \cot\beta - \mu$ can be large if the μ parameter is large. For $m_Q^2 \gg m_D^2$, the lightest sbottom state has mass

$$m_{\tilde{b}_1}^2 \approx m_D^2 + D_R^b - \frac{m_b^2 \tan^2\beta}{v^2} \frac{X_b^2}{m_Q^2} \phi^2 \quad \Rightarrow \quad \alpha_{\tilde{b}_1} = -\frac{m_b^2 \tan^2\beta}{v^2} \frac{X_b^2}{m_Q^2} < 0 . \tag{22}$$

For large $\tan\beta$ and μ, negative and sizable $\alpha_{\tilde{b}_1}$ can be obtained. Notice if such sbottom was present, the stop can be made heavier, so the danger of our universe may develop into the color breaking vacuum [17] is less severe.

B. Constraints in the MSSM

Here we show there is a series of constraints in the minimal model that prevent the above light sbottom assisted light stop scenario to work as designed at the beginning of this section.

First, at large field values, the zero-temperature potential is approximately

$$V(\phi, \tilde{b}_1) \approx \frac{\lambda}{4}\phi^4 - \alpha_{\tilde{b}_1}\phi^2 \tilde{b}_1^* \tilde{b}_1 + \kappa_{\tilde{b}_1}(\tilde{b}_1^* \tilde{b}_1)^2 . \tag{23}$$

For the potential to be bounded from below, we must require

$$\alpha_{\tilde{b}_1} > -\sqrt{\kappa_{\tilde{b}_1}\lambda} = -\sqrt{\frac{1}{6}\left(g_3^3 + \frac{1}{3}g_1^2\right) \cdot \frac{m_h^2}{2v^2}} \approx -0.2 . \tag{24}$$

Here the self interaction $\kappa_{\tilde{b}_1} = \kappa_{\tilde{b}_R} \approx 0.26$ is fixed by the gauge couplings from the $\tilde{b}_R$ D-terms. There is no room to enlarge it if MSSM is taken to be a complete theory.

The second but more severe tension arises from a combined consideration of Higgs mass and vacuum stability. In the MSSM, radiative corrections are crucial to lift the tree-level Higgs mass. Neglecting the stop mixing effect, we have [35]

$$(m_h^2)_{1-\text{loop}} \approx M_Z^2 \cos^2 2\beta + \frac{3G_F m_t^4}{\sqrt{2}\pi^2} \log \frac{m_{\tilde{t}_1} m_{\tilde{t}_2}}{m_t^2} . \tag{25}$$

In the light stop scenario $m_{\tilde{t}_1} < m_t$, in order to achieve $m_h = 125\,\text{GeV}$, the heavier stop must satisfy $m_{\tilde{t}_2} \approx m_Q \gtrsim 5\,\text{TeV}$. Since the two loop effects tend to decrease the Higgs mass, we need an even larger $m_Q > 10\,\text{TeV}$. We also consider the vacuum stability [36–39, 41] of the heavy $\tilde{b}_L$ field. Taking $\tilde{b}_L$ as a background field, there is a negative finite loop correction to its quartic interaction

$$\delta\kappa_{\tilde{b}_L} \approx -\frac{1}{32\pi^2}\frac{1}{6}\left(\frac{m_b \tan\beta}{v}\frac{X_b}{\tilde{m}}\right)^4 = -\frac{1}{192\pi^2}|\alpha_{\tilde{b}_1}|^2 \left(\frac{m_Q}{\tilde{m}}\right)^4 , \tag{26}$$

where $\tilde{m}$ is the mass scale of the particles running in the box diagram, h and $\tilde{b}_R$, both of which are lighter than $\sim 200\,\text{GeV}$ for our interest. In order not to develop a color breaking vacuum of $\tilde{b}_L$, this correction should be smaller than the tree-level coupling $\kappa_{\tilde{b}_L}^{\text{tree}} = g_3^2/6 + g_2^2/4 + g_1^2/72 \approx 0.36$. For $\alpha_{\tilde{b}_1} = -0.2$, this implies an upper bound, $m_Q \lesssim 2\,\text{TeV}$.

Interchanging the role of left and right-handed sfermion masses does not work either. In this case, the light stop and sbottom will share the same bare mass m_Q^2. The phase

transition requires $m_Q^2 \lesssim 0$ from the stop side, while the sbottom (with $\alpha_{\tilde{b}_1} < 0$) satisfying the LEP limit requires $m_Q^2 \gtrsim 100\,\text{GeV}$. Moreover, this case is also more constrained by the electroweak precision T parameter [40].

To summarize, the above discussions exclude $\alpha_{\tilde{b}_1}$ from being sizable, and reinforce the status that MSSM electroweak baryogenesis becomes disfavored after the Higgs discovery.

C. Possible solutions by going beyond

The above constraints could be evaded if the MSSM is regarded as an effective theory, plus the remnant effects from higher scale physics. Possible solutions to the vacuum stability problem include enhancing the self interactions of Higgs boson and $\tilde{b}_L$. If the $\tilde{b}_R$ self interaction is also enlarged, the lower bound in Eq. (24) can be further relaxed.

One may argue that the light stop window is less unique if one is allowed to go beyond MSSM. However, if the sbottom assisted light stop scenario were to work, a clear prediction would be very light third generation sfermions, which are testable even at the current stage of LHC, as emphasized in the next subsection.

The extra contributions to the Higgs mass allow the second stop mass m_Q to be substantially smaller, so the dangerous correction in Eq. (26) can be made safely small. The enhancement in the Higgs boson self-interaction widely exists in the extensions to the MSSM, from the F-term [41] such as the NMSSM and , or from a non-decoupled D-term [42–44] [45–47] (see also [48]). Here, we show an example following the discussion of supersymmetric left-right model in [44]. The gauge symmetry is $SU(2)_L \times SU(2)_R \times U(1)_{B-L}$ which breaks to SM gauge symmetry at a scale $v_R \gtrsim \text{TeV}$. In order to match to the SM D-terms in the supersymmetric decoupling limit, the tree-level exchange of the uneaten scalar component (real part) in the would-be Goldstone superfield is found to be crucial. Soft SUSY breaking mass terms violate its degeneracy with the heavy gauge bosons and gauginos. The correction to the Higgs self interaction is

$$2\delta\lambda_h = \frac{g_2^2 g_{BL}^2 + g_2^2 \frac{m^2}{v_R^2}}{g_2^2 + g_{BL}^2 + \frac{m^2}{v_R^2}} - g_1^2 \;, \tag{27}$$

where $g_{BL}^2 = g_2^2 g_1^2 / (g_2^2 - g_1^2)$, and m here is the soft SUSY breaking mass in the $SU(2)_R \times U(1)_{B-L}$ breaking Higgs sector. For $m^2/v_R^2 = 2$ and $m_{\tilde{t}_1} = 130\,\text{GeV}$, $m_{\tilde{t}_2} \approx m_Q \approx 2\,\text{TeV}$, we find $125\,\text{GeV}$ Higgs mass can be easily accommodated. This solves the second constraint discussed in Sec. IV B.

The self-interaction of sbottoms may be enhanced through the F-term by coupling them to new vector-like states. As an illustration, we introduce a pair of exotic states $X, \bar{X}$ and the corresponding superpotential $W = MX\bar{X} + \lambda' X b^c b^c$. After integrating out $X, \bar{X}$, there could be a correction to the $\tilde{b}_R$ self coupling, in the presence of soft SUSY breaking mass m of $\bar{X}$, $\delta\kappa_{\tilde{b}_R} = |\lambda'|^2 m^2/(M^2 + m^2)$. If $M \sim m$ and λ' is large, this helps to relax the first constraint above.

D. Light sbottom and stop at LHC

The main testable prediction from the above picture, is the existence of a light sbottom (below $200\,\text{GeV}$), and a relatively heavier light stop (can be as heavy as $140\,\text{GeV}$). The light

sbottom and stop can be directly and copiously produced at hadron colliders. This opens up further motivations for the urgency of their direct searches at the LHC in the near future.

Direct search has been regarded as a crucial test of the light stop scenario for EWBG. The current limits are summarized and discussed in [24, 49], which vary depending on the decay channels. For the stop mass below $< 150\,\mathrm{GeV}$, it mainly decays into $\tilde{t}_1 \to bW^+\tilde{\chi}_1^0$, via an off-shell chargino or top quark, where the dominant background from SM $t\bar{t}$ production. We observe there is no limit from Tevatron or LHC for a light stop whose mass is near to that of the lightest neutralino [50]. In this case, the lower limit comes from LEP, which is 96 GeV. The bound could get stronger when the mass difference between stop and neutralino is close enough to the co-annihilation regime and $\tilde{t}_1 \to c\tilde{\chi}_1^0$ takes over. It seems challenging to exclude the EWBG scenario by searching for the stop alone.

This gives more priority to look into the light sbottom direct searches, which is another prediction from the framework set up in this paper. A light sbottom could decay into a bottom quark and the lightest neutralino, $\tilde{b}_1 \to b\tilde{\chi}_1^0$. The current lower bound for this channel using events with two hard b-jets and missing energy can be as large as 400 GeV, for a very light neutralino [51]. However, this bound gets much weaker, down to $\sim 100\,\mathrm{GeV}$ when the mass difference between sbottom and neutralino are close. The monojet events are expected to play a complementary role [52, 53], and have the potential to cover the whole light sbottom region after the 8 TeV run of LHC [54]. The sbottom may also be longer lived than the collider time scale. In this case, it can also be tightly constrained by searching for events with displaced vertices or even stopped particles inside the detectors [55, 56].

V.   CONCLUSIONS

The discovery of a 125 GeV Higgs boson at LHC has led us into an era of precise measurement of Higgs couplings. This will finally give us deeper understanding of the EWSB and possible connections to new physics from the Higgs portal. We confront the new electroweak states that can trigger strong first order EWPT to the global fit of the current Higgs data. A close correlation exists between the two phenomena if such new states carry color and/or electric charge. It has been pointed out that a single scalar responsible for strong EWPT, such as a light stop in the MSSM, is in tension with the current Higgs fit.

In this work, we extend this minimal picture and study the possibility of having multiple new scalars present at the electroweak scale. We set up a general framework, in which a first scalar S_1 with positive Higgs portal coupling triggers the first-order phase transition, and a second scalar S_2 with similar mass but opposite Higgs coupling not only improves the Higgs fit, but also further enhances the strength of phase transition. This enables us to substantially improve the compatibility between the Higgs fit and EWPT, which we notice is essentially independent of how the first order EWPT is triggered. Accordingly, we expect the mechanism proposed here extremely intriguing, and widely applicable in almost all beyond SM models with a first order EWPT.

We have discussed possible realization of this framework in SUSY theories, including the MSSM and beyond. We realize the constraints in the MSSM from the color breaking vacua, and find they could be evaded by extending the minimal model. We show two examples where the Higgs boson and the squark self interactions can be enhanced through non-decoupled D-term and/or F-term. The prediction of both a light stop (around 140 GeV) and a light sbottom (below 200 GeV) is highlighted, and which can be directly tested at the LHC in the near future.

[1] G. Aad *et al.* [ATLAS Collaboration], Phys. Lett. B **716**, 1 (2012) [arXiv:1207.7214 [hep-ex]].

[2] S. Chatrchyan *et al.* [CMS Collaboration], Phys. Lett. B **716**, 30 (2012) [arXiv:1207.7235 [hep-ex]].

[3] B. Batell, S. Gori and L. -T. Wang, JHEP **1206**, 172 (2012) [arXiv:1112.5180 [hep-ph]].

[4] D. Carmi, A. Falkowski, E. Kuflik and T. Volansky, JHEP **1207**, 136 (2012) [arXiv:1202.3144 [hep-ph]].

[5] A. Azatov, R. Contino and J. Galloway, JHEP **1204**, 127 (2012) [arXiv:1202.3415 [hep-ph]].

[6] J. R. Espinosa, C. Grojean, M. Muhlleitner and M. Trott, JHEP **1205**, 097 (2012) [arXiv:1202.3697 [hep-ph]].

[7] P. P. Giardino, K. Kannike, M. Raidal and A. Strumia, JHEP **1206**, 117 (2012) [arXiv:1203.4254 [hep-ph]].

[8] I. Low, J. Lykken and G. Shaughnessy, arXiv:1207.1093 [hep-ph].

[9] P. P. Giardino, K. Kannike, M. Raidal and A. Strumia, arXiv:1207.1347 [hep-ph].

[10] T. Corbett, O. J. P. Eboli, J. Gonzalez-Fraile and M. C. Gonzalez-Garcia, arXiv:1207.1344 [hep-ph].

[11] J. R. Espinosa, C. Grojean, M. Muhlleitner and M. Trott, arXiv:1207.1717 [hep-ph].

[12] D. Carmi, A. Falkowski, E. Kuflik, T. Volansky and J. Zupan, arXiv:1207.1718 [hep-ph].

[13] T. Plehn and M. Rauch, arXiv:1207.6108 [hep-ph].

[14] V. A. Kuzmin, V. A. Rubakov and M. E. Shaposhnikov, Phys. Lett. B **155**, 36 (1985).

[15] Fermions with large yukawa couplings to Higgs can also trigger a strong first order EWPT if we consider their entropy production when they are decoupled. See [16]. Nevertheless, this mechanism requires some fine tuning of the Higgs potential and is not generic so we do not consider this possibility here.

[16] M. S. Carena, A. Megevand, M. Quiros and C. E. M. Wagner, Nucl. Phys. B **716** (2005) 319 [hep-ph/0410352].

[17] M. S. Carena, M. Quiros and C. E. M. Wagner, Phys. Lett. B **380**, 81 (1996) [hep-ph/9603420].

[18] There is an second possibility to fit the current Higgs data which flips the sign between the hgg and $h\gamma\gamma$ couplings, however, this possibility may suffer from vacuum stability, color breaking problems [36] and requires extremely negative α so it is irrelevant to strongly first order EWPT.

[19] D. J. H. Chung, A. J. Long and L. -T. Wang, arXiv:1209.1819 [hep-ph].

[20] A. G. Cohen and M. Schmaltz, arXiv:1207.3495 [hep-ph].

[21] M. Carena, G. Nardini, M. Quiros and C. E. M. Wagner, JHEP **1302**, 001 (2013) [arXiv:1207.6330 [hep-ph]].

[22] T. Cohen, D. E. Morrissey and A. Pierce, Phys. Rev. D **86**, 013009 (2012) [arXiv:1203.2924 [hep-ph]].

[23] D. Curtin, P. Jaiswal and P. Meade, JHEP **1208**, 005 (2012) [arXiv:1203.2932 [hep-ph]].

[24] M. Carena, I. Low and C. E. M. Wagner, JHEP **1208**, 060 (2012) [arXiv:1206.1082 [hep-ph]].

[25] M. Carena, G. Nardini, M. Quiros and C. E. M. Wagner, Nucl. Phys. B **812**, 243 (2009) [arXiv:0809.3760 [hep-ph]].

[26] M. Gillioz, R. Grober, C. Grojean, M. Muhlleitner and E. Salvioni, arXiv:1206.7120 [hep-ph].

[27] M. Quiros, hep-ph/9901312.

[28] T. A. Chowdhury, M. Nemevsek, G. Senjanovic and Y. Zhang, JCAP **1202**, 029 (2012) [arXiv:1110.5334 [hep-ph]].

[29] T. Cohen and A. Pierce, Phys. Rev. D **85**, 033006 (2012) [arXiv:1110.0482 [hep-ph]].

[30] H. H. Patel and M. J. Ramsey-Musolf, JHEP **1107**, 029 (2011) [arXiv:1101.4665 [hep-ph]].

[31] C. Wainwright, S. Profumo and M. J. Ramsey-Musolf, Phys. Rev. D **84**, 023521 (2011) [arXiv:1104.5487 [hep-ph]].

[32] C. L. Wainwright, S. Profumo and M. J. Ramsey-Musolf, arXiv:1204.5464 [hep-ph].

[33] J. M. Cline and P. -A. Lemieux, Phys. Rev. D **55**, 3873 (1997) [hep-ph/9609240].

[34] D. J. H. Chung, B. Garbrecht, M. J. Ramsey-Musolf and S. Tulin, Phys. Rev. Lett. **102** (2009) 061301 [arXiv:0808.1144 [hep-ph]].

[35] A. Djouadi, Phys. Rept. **459**, 1 (2008) [hep-ph/0503173].

[36] M. Reece, arXiv:1208.1765 [hep-ph].

[37] T. Kitahara, arXiv:1208.4792 [hep-ph].

[38] K. S. Babu and C. Macesanu, Phys. Rev. D **67**, 073010 (2003) [hep-ph/0212058].

[39] R. Sato, K. Tobioka and N. Yokozaki, Gauge Mediation Models," Phys. Lett. B **716**, 441 (2012) [arXiv:1208.2630 [hep-ph]].

[40] J. R. Espinosa, M. Quiros and F. Zwirner, Phys. Lett. B **307**, 106 (1993) [hep-ph/9303317].

[41] A. Delgado, G. Nardini and M. Quiros, JHEP **1204**, 137 (2012) [arXiv:1201.5164 [hep-ph]].

[42] P. Batra, A. Delgado, D. E. Kaplan and T. M. P. Tait, JHEP **0402**, 043 (2004) [hep-ph/0309149].

[43] A. Maloney, A. Pierce and J. G. Wacker, JHEP **0606**, 034 (2006) [hep-ph/0409127].

[44] Y. Zhang, H. An, X. -d. Ji and R. N. Mohapatra, Phys. Rev. D **78**, 011302 (2008) [arXiv:0804.0268 [hep-ph]].

[45] M. Endo, K. Hamaguchi, S. Iwamoto, K. Nakayama and N. Yokozaki, Phys. Rev. D **85**, 095006 (2012) [arXiv:1112.6412 [hep-ph]].

[46] C. Cheung and H. L. Roberts, arXiv:1207.0234 [hep-ph].

[47] H. An, T. Liu and L. -T. Wang, arXiv:1207.2473 [hep-ph].

[48] K. S. Babu, X. -G. He and E. Ma, Phys. Rev. D **36**, 878 (1987).

[49] G. Aad *et al.* [ATLAS Collaboration], arXiv:1209.2102 [hep-ex].

[50] http://indico.cern.ch/getFile.py/access?contribId=172&sessionId=65&resId=0&materialId=slides&confId=181298.

[51] G. Aad *et al.* [ATLAS Collaboration], Phys. Rev. Lett. **108**, 181802 (2012) [arXiv:1112.3832 [hep-ex]].

[52] T. Aaltonen *et al.* [CDF Collaboration], Phys. Rev. Lett. **108**, 211804 (2012) [arXiv:1203.0742 [hep-ex]].

[53] S. Chatrchyan *et al.* [CMS Collaboration], arXiv:1206.5663 [hep-ex].

[54] E. Alvarez and Y. Bai, JHEP **1208** (2012) 003 [arXiv:1204.5182 [hep-ph]].

[55] M. Fairbairn, A. C. Kraan, D. A. Milstead, T. Sjostrand, P. Z. Skands and T. Sloan, Phys. Rept. **438**, 1 (2007) [hep-ph/0611040].

[56] S. Chatrchyan *et al.* [CMS Collaboration], JHEP **1208**, 026 (2012) [arXiv:1207.0106 [hep-ex]].